Mol Biol Rep (2012) 39:3211–3218
DOI 10.1007/s11033-011-1088-4

Nacre-driven water-soluble factors promote wound healing of the deep burn porcine skin by recovering angiogenesis and fibroblast function

Kyunghee Lee · Hyunsoo Kim · Jin Man Kim · Yeoun Ho Chung · Tae Yoon Lee · Hyun-Sook Lim · Ji-Hye Lim · Taewoon Kim · Jin Seung Bae · Chang-Hoon Woo · Keuk-Jun Kim · Daewon Jeong

Received: 21 January 2011 / Accepted: 11 June 2011 / Published online: 19 June 2011

Abstract To assess the recovery effect of water-soluble components of nacre on wound healing of burns, water-soluble nacre (WSN) was obtained from powdered nacre. Alterations to WSN-mediated wound healing characteristics were examined in porcine skin with deep second-degree burns; porcine skin was used as a proxy for human. When WSN was applied to a burned area, the burn-induced granulation sites were rapidly filled with collagen, and the damaged dermis and epidermis were restored to the appearance of normal skin. WSN enhanced wound healing recovery properties for burn-induced apoptotic and necrotic cellular damage and spurred angiogenesis. Additionally, WSN-treated murine fibroblast NIH3T3 cells showed increased proliferation and collagen synthesis. Collectively, the findings indicate that WSN improves the process of wound healing in burns by expeditiously restoring angiogenesis and fibroblast activity. WSN may be useful as a therapeutic agent, with superior biocompatibility to powdered nacre, and evoking less discomfort when applied to a wounded area.

Keywords Nacre · Water-soluble factor · Burn injury · Skin regeneration · Wound healing

K. Lee and H. Kim contributed equally to this study.

K. Lee · H. Kim · J. M. Kim · Y. H. Chung · T. Y. Lee · D. Jeong (✉)
Department of Microbiology, Yeungnam University College of Medicine, Daegu 705-717, Korea
e-mail: dwjeong@ynu.ac.kr

H.-S. Lim
Department of Public Health Administration, Hanyang Women's University, Seoul 133-793, Korea

J.-H. Lim
Department of Health and Medical Administration, Dongju College University, Busan 604-715, Korea

T. Kim
Rion Technology, Bio-industrial Center, JIB, Jeonju 561-360, Korea

J. S. Bae
Uiseong Oriental Medicine Hospital, Uiseong-Gun 1137-18, Korea

C.-H. Woo
Department of Pharmacology, Yeungnam University College of Medicine, Daegu 705-717, Korea

K.-J. Kim
Department of Clinical Pathology, Taekyeung College, Gyeungsan 712-719, Korea

Introduction

The skin is a dynamic and integrated organ with the largest surface area in the human body. Its diverse functions include protection from infectious microorganisms and ultraviolet radiation, permeability barrier to block water loss, thermoregulation, and sensation [1, 2]. These normal functions can be gradually decreased by many factors, such as aging, health status, and environmental pollutants, and can be suddenly and catastrophically affected by severe wounds including chronic ulcers and burns [3, 4].

Although the severity of wounded skin differs according to its area and depth, burns have the potential to cause the loss of sensation and joint mobility, anatomic deformity, and death [5, 6]. Burns generally consist of superficial (first-degree) burns that include the injury to the epidermis, deep partial thickness (second-degree) burns that include damage to the reticular layer of the dermis,

and full thickness (third-degree) burns that include damage to the entire dermis [7]. Generally, the sequential processes of wound healing are denaturation and necrosis of wounded tissues, inflammation, angiogenesis, liquefaction, and discharge of the denatured and necrotic tissues via fibroblast-produced granulation tissue formation, and tissue remodeling by the restoration of physiological structure and function [8, 9]. Much clinical investigation has focused on prompt wound healing of damaged skin including burns and the retardation of skin degeneration process caused by aging and exposure to dangerous environmental factors.

Nacre, also called mother of pearl, occurs naturally as the iridescent internal layer of mollusk shells. It consists of 95% inorganic components including calcium carbonate ($CaCO_3$) of the aragonite form, and 5% organic matrix [10, 11]. Nacre is effective in maintaining normal healthy skin and in facilitating the regeneration of wounded skin. These beneficial properties have been known for a long time; nacre is the basis of a traditional medicine to treat skin wounds resulting from conditions including decubitus ulcer and as a cosmetic material to improve the reduced functional activity of skin. Despite these uses and their long history, there is no clinical data regarding the role of nacre in skin regeneration and wound healing in vitro and in vivo; the prowess of nacre in treating decubitus ulcer is based on the anecdotal report of an experienced doctor of oriental medicine.

The present study assessed the wound healing capabilities of nacre-driven water-soluble components (water-soluble nacre, WSN) at the cellular level in a porcine model of deep second-degree burn. The results indicate that WSN can improve wound healing through the prompt recovery of angiogenesis, fibroblast proliferation, and collagen synthesis. Especially, considering its diffusible efficiency and circulation through the body, WSN may have merit in the development of biocompatible and applicable products that are more useful for treatment of wound healing than powdered nacre.

Materials and methods

Materials

Formaldehyde was purchased from Bio Basic (Markham, ON, Canada). Trypan blue solution and bovine serum albumin (BSA) were purchased from Invitrogen (Carlsbad, CA). Fibronectin and crystal violet were purchased from Sigma-Aldrich (St. Louis, MO). Water was of Milli Q grade. All other reagents were of the highest commercial grade available.

Preparation of WSN

Powdered nacre with fine pore size (<100 μm) was obtained from the inner shell layer of the pearl oyster *Pteria martensii*. The powder was suspended in ultra-pure water in a final concentration of 0.4% (w/v) and extracted for 12 h at room temperature with rocking. After centrifugation at 3,000×*g*, the resulting WSN was sterilized by passage through a 0.22 μm pore size filter and sprayed directly on the wounded site. Additionally, a powdered form of WSN was suspended in a 1:2 mixture of powder (weight) and ultra-pure water (volume). Cells were treated with WSN of a final concentration of 25 mg/ml.

Burn model

Five-month-old, two *Sus scrofa domesticus* female porcines (PWG MICRO-PIG®) were purchased from PWG (Seoul, Korea). Following general anesthesia to minimize the pain, the dorsal fur was shaved and a 3 cm^2 square rigid aluminum bar was adhered closely to the dorsal skin. The bar was exposed to water at 95°C for 15 s, resulting in deep second-degree burn wounds. WSN (0.4%, w/v) was directly sprayed on the skin injury at 2-day intervals for 35 days after burning. In vivo experiments were performed in triplicate per group, using two independent porcines. The animals were treated according to guidelines approved by the Institutional Animal Care and Use Committee of the Yeungnam University Medical School.

Histological assessment

Specimens fixed with formaldehyde were embedded in paraffin, sectioned at a thickness of 4 μm, and deparaffinized. To observe the change of granulation parts and fibroblast populations caused by burns, specimens were stained with hematoxylin and eosin (HE). To assess cell damage, cells with the fragmented chromosomal DNA were detected using TUNEL staining according to the manufacturer's protocols (In Situ Apoptosis Detection Kit; Intergen, Burlington, MA) and by counter staining with Mayer's hematoxylin. In addition, collagen distribution and endothelial cells in blood vessels were determined by immunohistological probing with a mouse monoclonal antibody to type I collagen (Novus Biologicals, Littleton, CO) and a rabbit polyclonal antibody to factor VIII (Biocare Medical, Concord, CA), respectively, by visualizing with Polink-2 HRP Plus Broad DAB Detection System (Golden Bridge International, Mukilteo, WA), and by counter staining with Mayer's hematoxylin. All photographs of specimens were taken using a ScanScope XT System (Aperio Technologies, Vista, CA).

Cell culture and proliferation

Murine fibroblast NIH3T3 cell line was cultured in a humidified atmosphere of 5% CO_2/95% air, at 37°C in Dulbecco's Modified Eagle's Medium (DMEM; Hyclone, Logan, UT) containing 10% fetal bovine serum (FBS; Hyclone), 100 U/ml penicillin, and 100 μg/ml streptomycin (Hyclone). Cells (2×10^4 cells/ml) were seeded in wells of a 24-well culture plate and incubated in the absence and presence (25 mg/ml) WSN for designated times. The number of viable cells was counted using a standard trypan blue-exclusion method.

Cell migration

Cell migration was assessed in two ways. To perform the scratch migration assay, NIH3T3 cells were grown to confluence and the confluent layer was scratched. Migration of cells into the scratch was determined by measuring the length of the gap with time. Additionally, cell migration was examined using a Transwell chamber (Corning, NY) as previously described [12], with some modifications. Briefly, after cells were suspended in serum-free DMEM supplemented with 0.5% FBS and 0.1% bovine serum albumin (BSA), 3×10^4 cells in 100 μl were seeded in each fibronectin (0.05 μg/ml)-coated top chamber of a Transwell apparatus. The lower chambers contained 600 μl of serum-free DMEM alone or with 25 mg/ml of WSN. Cells were allowed to migrate for 5 h, followed by fixation with formaldehyde and staining with crystal violet. Cells that had not migrated to the lower chamber were removed from the top chamber surface using a cotton swab. Cells that had migrated to the surface of the lower chamber were counted using a light microscope.

Reverse transcription polymerase chain reaction (RT-PCR)

NIH3T3 cells cultured to 70% confluence were treated with WSN for 1 or 2 days before total RNA extraction with Trizol (Invitrogen); Total RNA (2 μg) were then reverse-transcribed using Moloney Murine Leukemia Virus Reverse Transcriptase (Promega, Madison, WI), with oligo dT, at 42°C for 1 h. The primers used for PCR amplification were as follows: type I col1agen, sense: 5′-GACGCCATCAAGGTCTACTG-3′, and antisense: 5′-ACGGGAATCCATCGGTCA-3′; glyceraldehyde 3-phosphate dehydrogenase (GAPDH), sense: 5′-CAAGGCTGTGGGCAAGGTCA-3′, and antisense: 5′-GCAACTCCCACTCTTCCACCT-3′.

Western blotting analysis

NIH3T3 cells that had grown to 70% confluence were treated with WSN and further incubated for 2 days. Total cell lysates were fractionated by 10% sodium dodecyl sulfate polyacrylamide gel electrophoresis (SDS-PAGE). The resolved proteins were transferred to a nitrocellulose membrane (Whatman GmbH, Hahnestrabe, Dassel, Germany) and probed with a goat polyclonal antibody to collagen type I (Santa Cruz Biotechnology, Santa Cruz, CA) and mouse monoclonal antibody to β-actin (Sigma-Aldrich). The blot was then probed with appropriate horseradish peroxidase-conjugated second antibody and developed by enhanced chemiluminescence reagents (Lab Frontier, Seoul, Korea).

Statistical analysis

Data are expressed as the mean ± SD ($n = 3$). Means between two groups were compared using the Student's t-test with a 95% confidence.

Results

WSN-mediated histological changes in skin wound regeneration

Since porcine skin is morphologically and functionally similar to human skin [13], a deep second-degree burn porcine model was developed to evaluate the effect of WSN on wound healing in skin. The initial investigation focused on wound healing indexes, including the number of necrotic damaged cells, angiogenesis, and granulation and collagen tissue distribution on post-burn day 35. WSN induced a small remnant of granulation tissues compared to water-treated control (Fig. 1). This likely reflected an increased wound healing process due to the prompt elimination of granulation tissues at the base of the wound site. As shown in Fig. 2, WSN reduced the population of burn-induced apoptotic and necrotic damaged cells, which is characterized by terminal deoxynucleotidyl transferase-mediated dUTP nick end labeling (TUNEL) staining, and displayed a tendency to lessen blood-vessel dilation during the wound healing process, which is determined by detecting factor VIII expressed on endothelial cells of blood vessel. Also, WSN-treated wound sites contained dense collagen tissue compared to water-treated control wound sites. It is well-known that the clearance of necrotic tissue, formation of new blood vessels, granulation tissue formation, and collagen synthesis by fibroblasts are critical

steps in the wound healing process [8, 9]. Our findings indicate that WSN can facilitate these various wound healing processes.

WSN stimulation of fibroblast proliferation and extracellular matrix synthesis

Dermal fibroblasts play a critical role in dermal wound healing [14, 15]. These cells proliferate and migrate into the bottom of a wound site and then synthesize new matrix proteins including collagen. We therefore counted the number of fibroblasts appearing at granulation sites. WSN treatment increased the number of fibroblasts in burn-induced granulation sites to a level similar to that seen in normal skin (Fig. 3), suggesting that fibroblast proliferation in WSN-treated tissue outpaced that in untreated burned tissue, thereby accelerating wound remodeling. Fibroblast recruitment to WSN-exposed healing burns was also more rapid than that in untreated burned controls; these fibroblasts, however, quickly dispersed as healing progressed.

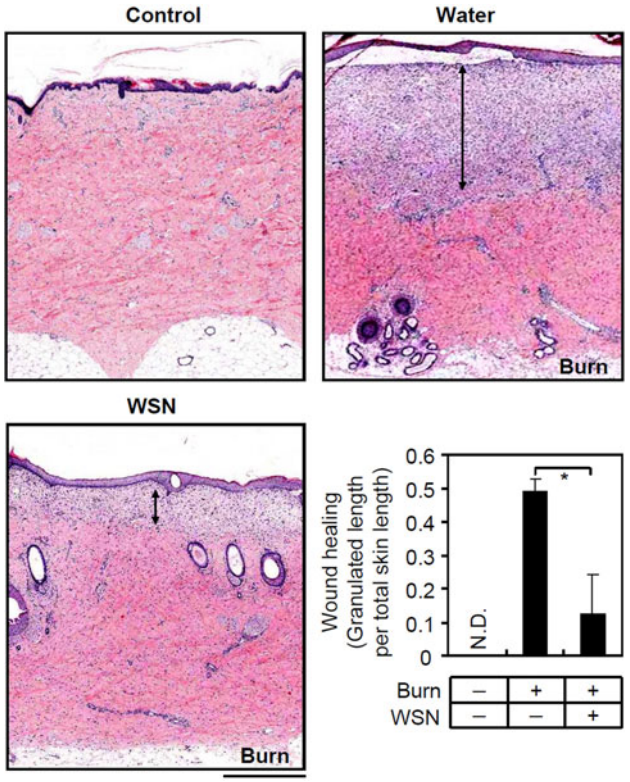

Fig. 1 Recovery effect of WSN on burn-wounded granulation tissue. Under anesthesia, deep dorsal second-degree burns were formed in porcines. Water as a control and WSN were directly sprayed on the wounded area at 2-day intervals for 35 days. Biopsy of the full-thickness skin was performed under anesthesia. Biopsied tissue was embedded in paraffin, sectioned, deparaffinized and stained with HE, after which the length of granulation tissue was measured. Data are expressed as the mean ± SD of experiments performed in triplicate. $^{*}P < 0.01$. *ND* not detected. *Scale bar* 1 mm

WSN treatment therefore appears to stimulate wound healing by attracting fibroblasts to injured sites. As the presence of WSN was associated with fast granulation tissue formation, dense collagen tissues, and increased fibroblast proliferation (Figs. 1–3), an experiment attempted to assess whether WSN improved cell migration, proliferation, and collagen synthesis in fibroblast cultures in vitro. In WSN-treated samples, the gaps between cells in scratch-wounded monolayers quickly filled (Fig. 4a). This result could be caused by enhanced cell proliferation and/or increased cell migration. To clarify the phenomenon, cell proliferation was examined using a trypan blue exclusion assay and cell migration using a Transwell chamber assay. WSN stimulated fibroblast proliferation (Fig. 4b), but did not affect fibroblast migration (Fig. 4c). The accelerated wound healing process by WSN is thought to potentiate fibroblast proliferation. As shown in Fig. 4a and b, fibroblast proliferation was slightly increased by treatment with calcium of a final concentration of 14 μM, which was the same concentration of calcium dissolved in WSN (25 mg/ml). This observation indicates that calcium, one of many components in WSN, can enhance partially wound healing via the stimulation of fibroblast proliferation. Because collagen deposition is an essential component in the wound healing process [16–18], the effect of WSN on collagen production of fibroblasts was investigated. When fibroblasts were treated with WSN, this induced increased collagen expression at the level of mRNA and intracellular/secreted protein in a dose-dependent manner (Fig. 5), consistent with a more dense collagen distribution in WSN-treated tissue than in water-treated control tissue, as indicated in Fig. 2. It was also observed that calcium itself could facilitate collagen gene expression in fibroblasts and WSN displayed a synergistic action in collagen synthesis compared to calcium alone, indicating that WSN contains calcium as well as other additive molecules to potentiate collagen deposition in the wound healing process.

Discussion

Although there is no clinical evidence for the stimulatory action of nacre in skin regeneration, nacre is used widely and traditionally as a cosmetic material and a bedsore treatment. The present study investigated whether nacre is an effective constituent in wound healing and the mechanisms underlying WSN-mediated wound healing process.

The normal skin consists of epidermis and dermis and maintains steady-state equilibrium between two compositions. After injury to the skin, the wound healing process is orchestrated by sequential or overlapped cascade reactions [8, 9]. Inflammation, which begins immediately in the early phase of wound healing, is essential for removing damaged

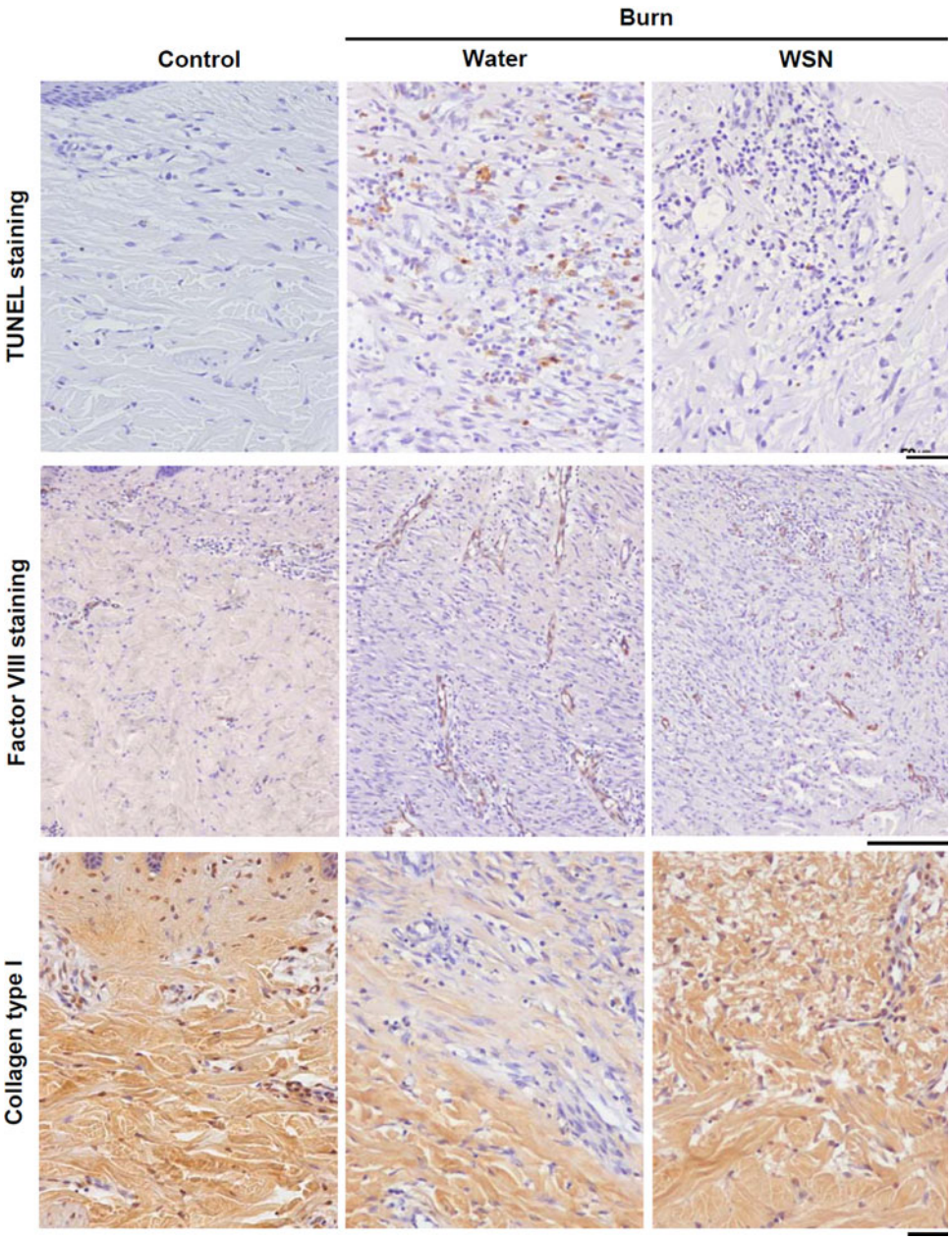

Fig. 2 Histological assessment of wound healing. Paraffin-embedded skin was sectioned, deparaffinized and examined using a TUNEL assay to detect apoptotic and necrotic damaged cells (*upper panel*). Blood vessels with endothelial cells (*middle panel*) and collagen distribution (*lower panel*) were visualized by treatment of the specific antibodies to factor VIII and type I collagen, respectively. *Scale bar* 50 μm

tissue debris and infected bacteria. Next, the sequential proliferative phase is executed by epithelialization, angiogenesis, and apoptosis of unwanted cells, and granulation tissue formation by the connection of collagen, fibronectin, elastin, and other factors, which are secreted from fibroblasts. The process is followed by the remodeling through collagen cross-linking and reorganization. When most skin wounds are naturally and therapeutically healed, it is difficult to achieve a result that is aesthetically and functionally perfect. The final aim of wound healing is to rapidly and efficiently achieve complete healing. Among many natural materials to reduce skin degeneration, nacre has a long history as a traditional remedy to improve skin function. The present findings provide clear evidence that WSN facilitates wound healing in a deep second-degree burn porcine model by accelerated angiogenesis, shift in the ratio of resting to proliferating fibroblasts, and enhanced collagen synthesis of fibroblasts, which results in the efficient and prompt acceleration of granulation tissue formation and wound repair. These results are in agreement with the previous anecdotal observations of an experienced oriental doctor concerning the efficacy of WSN in treatment of bedsores.

Nacreous mother-of-pearl consists of 95–99% $CaCO_3$ and 1–5% organic components [10, 11]. A previous study

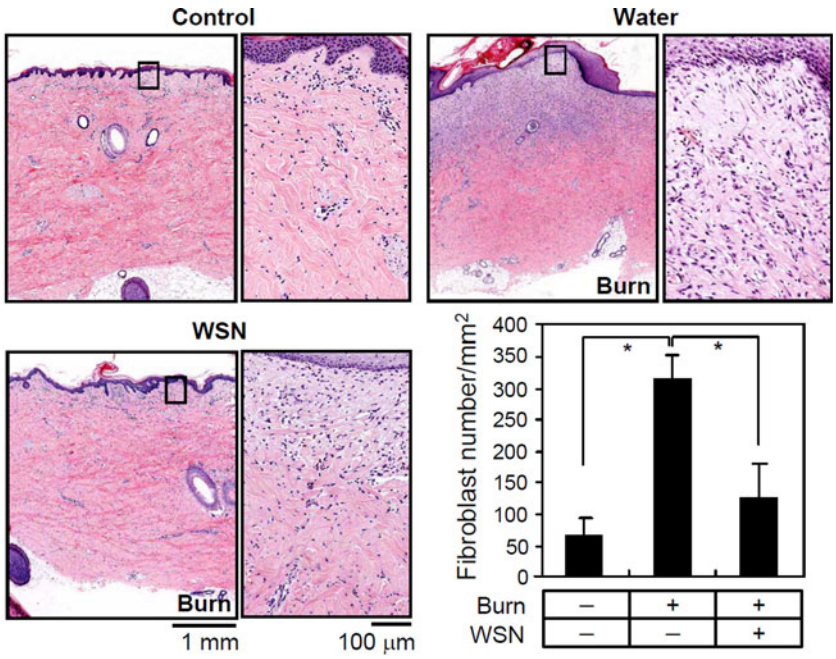

Fig. 3 Effect of WSN on fibroblast proliferation in burn-wounds. After specimens obtained as described in Fig. 1 were stained with HE and photographed, the number of epidermal and dermal fibroblasts was counted. *Small box* of the *left panel* is enlarged in the *right panel*. Data represent the mean ±SD of experiments performed in triplicate. $*P < 0.01$

has reported that nacre contains a number of biologically active entities of disparate molecular weight, including both inorganic minerals and organic proteins. Small molecules ranging from 50 to 235 Da can be fractionated from nacre, and are known to be capable of stimulating the osteogenic capacity of osteoblasts [19]. Unlike known osteogenic factors, which are usually of low molecular weight, water-soluble nacre matrix proteins of relatively high molecular weight can play a functional role in bone formation by osteoblasts and synthesis of fibrous matrix proteins by fibroblasts [20–24]. As nacre implanted into bone biodegrades, the implant region recovers through local acceleration of osteogenesis with biocompatible integration of the two heterogeneous nacre and bone [25–27]. When a mixture of nacre powder and autologous blood is implanted into rat dermis, skin fibroblasts are recruited adjacent to the implant area and produce extracellular matrix proteins that can potentiate cell adhesion and migration, eventually leading to rapid healing of the implanted area [20–22, 28]. It has further been reported that several matrix proteins are involved in determining both the structure and texture of nacre and in forming aragonite crystals during biomineralization of the shell [29–36]. Since nacre is presumed to contain the diffusible bioactive factors that induce tissue regeneration, WSN used in this study is likely to contain water-soluble wound-healing factors spanning a range of molecular weights, from small inorganic and organic compounds to large matrix proteins.

In the present study, an analysis of the water-soluble fraction extracted from nacre at a concentration of 500 mg/ml found that this fraction includes about 280 μg/ml proteins and a number of minerals, including calcium, potassium, sodium, magnesium, and zinc (data not shown). Based on our and others' data, WSN-mediated wound healing in a porcine skin model with deep second-degree burns is achieved via several routes. First, the water-soluble proteins extant within WSN can simulate extracellular matrix, and will directly stimulate adhesion, proliferation, and migration of the cells that participate in swift wound healing. Secondly, recognition of large matrix proteins or unknown stimuli by their cognate partners present on the cytoplasmic membrane of cells may induce the activation of signaling molecules involved in the de novo synthesis of proteins, including collagen, that will participate in wound healing: our findings were consistent with WSN-mediated acceleration of collagen deposition within a burn site and type I collagen synthesis in NIH3T3 fibroblast cells. Thirdly, WSN is predicted to contain low-molecular weight factors that can freely diffuse into cells to evoke skin regeneration and burn healing. Our data showed that a calcium control prepared from $CaCO_3$ could facilitate fibroblast proliferation and type I collagen synthesis. As the WSN used here was prepared without decalcification, it likely contained minerals such as calcium, which is essential to maintain normal cellular physiology, in addition to water-soluble matrix proteins. Finally, our observations indicate that nacre's ability to heal wounds is

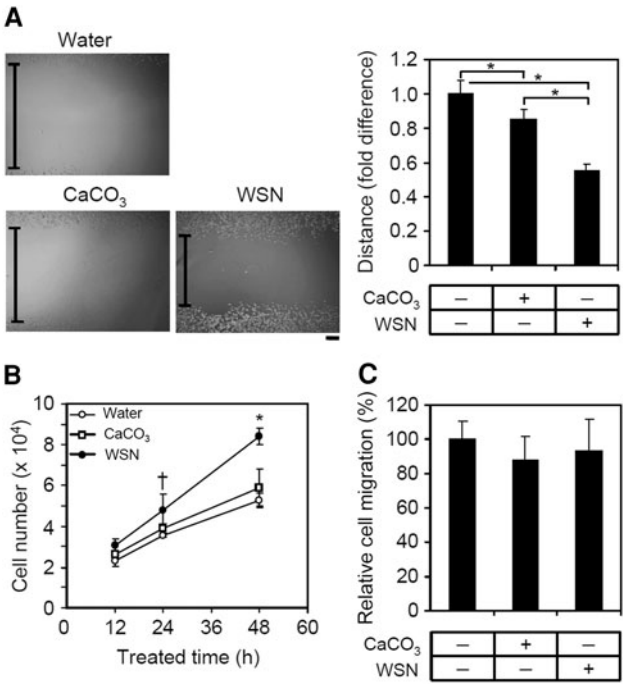

Fig. 4 Effects of WSN on cell migration and proliferation. **a** Scratch migration assay. After a scratch was made in confluent NIH3T3 cell growth, cells were further incubated in the absence or presence of WSN (25 mg/ml) for 12 h and changes in gap dimension were determined from measurements of images. Since 25 mg/ml WSN contains 14 μM calcium and $CaCO_3$ is known to be partially water-soluble [37], an identical concentration of calcium dissolved from $CaCO_3$ was used as a control to exclude the effect of calcium on wound healing. **b** Proliferation assay. NIH3T3 cells were treated without and with WSN for the indicated times and stained with trypan blue, after which trypan blue-excluded viable cells were counted under a microscope. **c** Transwell migration assay. After cells were seeded into fibronectin-coated top chambers of a Transwell apparatus and incubated for 5 h, the cells migrating to the lower chamber were counted. Data are expressed as the mean ± SD of a representative experiment performed in triplicate. $^{*}P < 0.01$; $^{\dagger}P < 0.05$. *Scale bar* 200 μm

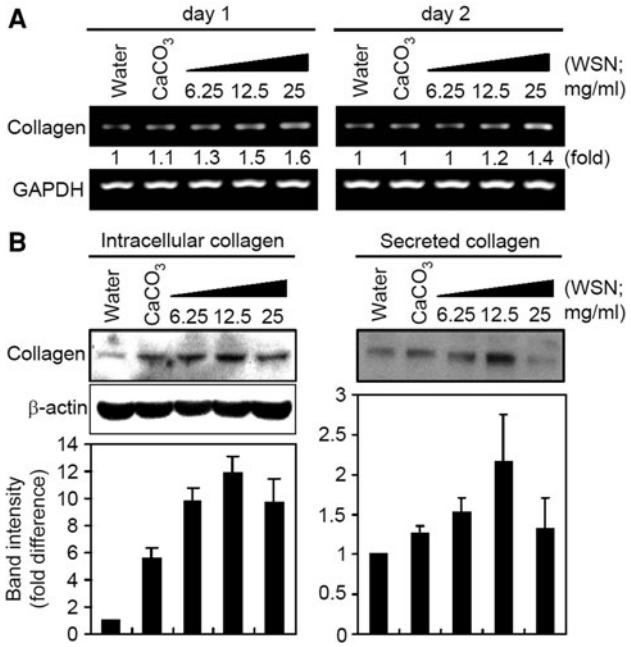

Fig. 5 Stimulatory effect of WSN on collagen synthesis in fibroblasts. NIH 3T3 cells were treated with WSN from 0 to 25 mg/ml for 2 days. **a** RT-PCR to detect collagen type I mRNA. After cells were harvested at the times indicated, the level of collagen type I mRNA was determined by RT-PCR. The indicated values represent fold change relative to the band intensity of the control; GAPDH was used to normalize mRNA levels. **b** Western blot analysis to detect intracellular and secreted collagen. Whole cell lysates and cultured media were fractionated by a 10% SDS-PAGE and the resolved proteins were transferred onto a nitrocellulose membrane. The level of collagen gene expression was determined by Western blotting with an antibody specific to collagen type I. The membrane was reprobed with antibody to *β*-actin to confirm the same protein loading. The values are expressed as a proportion of the control value. Data are expressed as the mean ± SD of at least three independent experiments

achieved by the combined effect of calcium and other soluble factors that are as yet uncharacterized.

The screening of a possible component(s) that mediates wound healing in WSN may be critical for developing wound dressings and therapeutic agents. We anticipate that WSN will accelerate the healing of burn injury by synergic inorganic/inorganic, organic/organic, or organic/inorganic mechanisms. The present observations indicate that WSN has therapeutic merit compared with powdered nacre in aspects that include vein, muscle, and oral routes of injection, efficient diffusion, and a broad biocompatible range from the skin to internal organs. In this regard, WSN may be more suitable than powdered nacre for developing various therapeutic products (e.g., ointments and wound dressings) to treat skin injury and cosmetic materials to maintain healthy skin from aging, sunlight, and environmental pollutants.

Acknowledgments This study was supported by a grant from the Korea Healthcare Technology R&D Project, Ministry for Health, Welfare and Family Affairs, Republic of Korea (A084221; to D. Jeong).

References

1. Proksch E, Brandner JM, Jensen JM (2008) The skin: an indispensable barrier. Exp Dermatol 17:1063–1072
2. Stander S, Schneider SW, Weishaupt C, Luger TA, Misery L (2009) Putative neuronal mechanisms of sensitive skin. Exp Dermatol 18:417–423
3. Raffetto JD (2009) Dermal pathology, cellular biology, and inflammation in chronic venous disease. Thromb Res 123(Suppl 4):S66–S71
4. Brigham PA, McLoughlin E (1996) Burn incidence and medical care use in the United States: estimates, trends, and data sources. J Burn Care Rehabil 17:95–107
5. Harrison CA, MacNeil S (2008) The mechanism of skin graft contraction: an update on current research and potential future therapies. Burns 34:153–163

6. Kealey GP, Jensen KT (1988) Aggressive approach to physical therapy management of the burned hand. A clinical report. Phys Ther 68:683–685
7. Ward RS, Saffle JR (1995) Topical agents in burn and wound care. Phys Ther 75:526–538
8. Shaw TJ, Martin P (2009) Wound repair at a glance. J Cell Sci 122:3209–3213
9. Clark RA (1993) Biology of dermal wound repair. Dermatol Clin 11:647–666
10. Levi-Kalisman Y, Falini G, Addadi L, Weiner S (2001) Structure of the nacreous organic matrix of a bivalve mollusk shell examined in the hydrated state using cryo-TEM. J Struct Biol 135:8–17
11. Weiner S (1986) Organization of extracellularly mineralized tissues: a comparative study of biological crystal growth. CRC Crit Rev Biochem 20:365–408
12. Sugatani T, Alvarez U, Hruska KA (2003) PTEN regulates RANKL- and osteopontin-stimulated signal transduction during osteoclast differentiation and cell motility. J Biol Chem 278:5001–5008
13. Sullivan TP, Eaglstein WH, Davis SC, Mertz P (2001) The pig as a model for human wound healing. Wound Repair Regen 9:66–76
14. Le Pillouer-Prost A (2003) Fibroblasts: what's new in cellular biology? J Cosmet Laser Ther 5:232–238
15. Gosain A, DiPietro LA (2004) Aging and wound healing. World J Surg 28:321–326
16. Rumalla VK, Borah GL (2001) Cytokines, growth factors, and plastic surgery. Plast Reconstr Surg 108:719–733
17. Switzer BR, Summer GK (1972) Collagen synthesis in human skin fibroblasts: effects of ascorbate, -ketoglutarate and ferrous ion on proline hydroxylation. J Nutr 102:721–728
18. Zhang GY, Gao WY, Li X, Yi CG, Zheng Y, Li Y, Xiao B, Ma XJ, Yan L, Lu KH, Han Y, Guo SZ (2009) Effect of camptothecin on collagen synthesis in fibroblasts from patients with keloid. Ann Plast Surg 63:94–99
19. Rousseau M, Boulzaguet H, Biagianti J, Duplat D, Milet C, Lopez E, Bedouet L (2008) Low molecular weight molecules of oyster nacre induce mineralization of the MC3T3–E1 cells. J Biomed Mater Res A 85:487–497
20. Lopez E, Le Faou A, Borzeix S, Berland S (2000) Stimulation of rat cutaneous fibroblasts and their synthetic activity by implants of powdered nacre (mother of pearl). Tissue Cell 32:95–101
21. Lopez E, Vidal B, Berland S, Camprasse S, Camprasse G, Silve C (1992) Demonstration of the capacity of nacre to induce bone formation by human osteoblasts maintained in vitro. Tissue Cell 24:667–679
22. Silve C, Lopez E, Vidal B, Smith DC, Camprasse S, Camprasse G, Couly G (1992) Nacre initiates biomineralization by human osteoblasts maintained in vitro. Calcif Tissue Int 51:363–369
23. Mouries LP, Almeida MJ, Milet C, Berland S, Lopez E (2002) Bioactivity of nacre water-soluble organic matrix from the bivalve mollusk *Pinctada maxima* in three mammalian cell types: fibroblasts, bone marrow stromal cells and osteoblasts. Comp Biochem Physiol B 132:217–229
24. Rousseau M, Pereira-Mouries L, Almeida MJ, Milet C, Lopez E (2003) The water-soluble matrix fraction from the nacre of *Pinctada maxima* produces earlier mineralization of MC3T3–E1 mouse pre-osteoblasts. Comp Biochem Physiol B 135:1–7
25. Liao H, Brandsten C, Lundmark C, Wurtz T, Li J (1997) Responses of bone to titania-hydroxyapatite composite and nacreous implants: a preliminary comparison by in situ hybridization. J Mater Sci Mater Med 8:823–827
26. Liao H, Mutvei H, Sjostrom M, Hammarstrom L, Li J (2000) Tissue responses to natural aragonite (margaritifera shell) implants in vivo. Biomaterials 21:457–468
27. Bahar H, Yaffe A, Binderman I (2003) The influence of nacre surface and its modification on bone apposition: a bone development model in rats. J Periodontol 74:366–371
28. Westbroek P, Marin F (1998) A marriage of bone and nacre. Nature 392:861–862
29. Marin F, Luquet G, Marie B, Medakovic D (2008) Molluscan shell proteins: primary structure, origin, and evolution. Curr Top Dev Biol 80:209–276
30. Suzuki M, Saruwatari K, Kogure T, Yamamoto Y, Nishimura T, Kato T, Nagasawa H (2009) An acidic matrix protein, Pif, is a key macromolecule for nacre formation. Science 325:1388–1390
31. Shen X, Belcher AM, Hansma PK, Stucky GD, Morse DE (1997) Molecular cloning and characterization of lustrin A, a matrix protein from shell and pearl nacre of *Haliotis rufescens*. J Biol Chem 272:32472–32481
32. Yano M, Nagai K, Morimoto K, Miyamoto H (2006) Shematrin: a family of glycine-rich structural proteins in the shell of the pearl oyster *Pinctada fucata*. Comp Biochem Physiol B 144:254–262
33. Miyashita T, Takagi R, Okushima M, Nakano S, Miyamoto H, Nishikawa E, Matsushiro A (2000) Complementary DNA cloning and characterization of Pearlin, a new class of matrix protein in the nacreous layer of oyster pearls. Mar Biotechnol (NY) 2:409–418
34. Zhang C, Li S, Ma Z, Xie L, Zhang R (2006) A novel matrix protein p10 from the nacre of pearl oyster (*Pinctada fucata*) and its effects on both CaCO3 crystal formation and mineralogenic cells. Mar Biotechnol (NY) 8:624–633
35. Zhang Y, Xie L, Meng Q, Jiang T, Pu R, Chen L, Zhang R (2003) A novel matrix protein participating in the nacre framework formation of pearl oyster, *Pinctada fucata*. Comp Biochem Physiol B 135:565–573
36. Xiong X, Chen L, Li Y, Xie L, Zhang R (2006) Pf-ALMP, a novel astacin-like metalloproteinase with cysteine arrays, is abundant in hemocytes of pearl oyster *Pinctada fucata*. Biochim Biophys Acta 1759:526–534
37. Feely RA, Sabine CL, Lee K, Berelson W, Kleypas J, Fabry VJ, Millero FJ (2004) Impact of anthropogenic CO2 on the CaCO3 system in the oceans. Science 305:362–366